

# Chapter 2 Experimental Apparatus

## 2.1 Vacuum System

In this experiment, STM and NC-AFM measurements were performed in ultra-high vacuum (UHV) chamber with a base pressure of  $8 \times 10^{-11}$  torr and equipped with a commercial variable-temperature STM/NC-AFM system. The UHV system consists of a scroll pump, two turbo pump, a titanium sublimation pump (TSP), and an ion pump.

The chamber is parted into three chambers; Loading chamber, Preparative chamber, and Observation chamber as shown in Fig. 2.1. The tips and samples were placed into the Loading chamber, and heated the loading chamber to  $\sim 120^\circ\text{C}$  for 16 hrs in purpose of separating the gas and moisture. Next, let the Loading cool off, and then transport the tips and samples to the preparative chamber. Various treatments will be treated depending upon the type of sample used in the experiment. Finally, the sample was measured in the observation chamber using STM or NC-AFM.

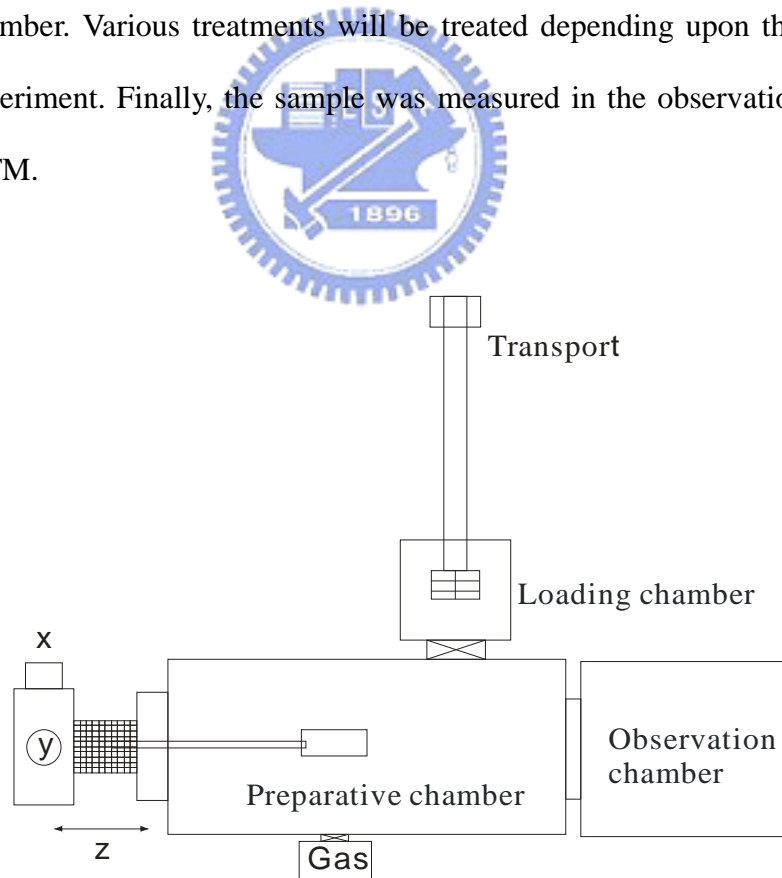


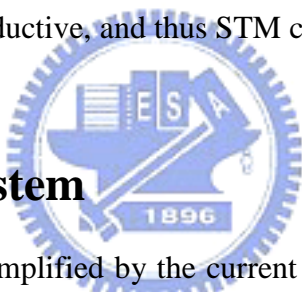
Fig. 2.1 Two-dimensional diagram that illustrates the chamber consisting of loading chamber, preparative chamber, and observation chamber.

## 2.2 Scanning Tunneling Microscopy (STM)

### 2.2.1 Introduction

Scanning Tunneling Microscope (STM) was invented in 1981 by G. Binnig and H Rohrer who shared the 1986 Nobel Prize in Physics for their invention. STM uses a sharp conducting tip and applies with a bias voltage between the tip and the sample. When the tip is brought close to the sample electrons can "tunnel" through the narrow gap either from the sample to the tip or vice versa, depending upon the induction of the bias voltage. This tunneling current changes with tip-to-sample distance, it decays exponentially with the distance, which gives STM its remarkably high precision in positioning the tip (sub-angstrom vertically and atomic resolution laterally). For the electron tunneling to take place, both the sample and the tip must be conductive, and thus STM cannot be used on insulating materials.

### 2.2.2 Feedback system



The tunneling current is amplified by the current amplifier to become a voltage ( $\Delta I-\Delta V$  transfer), which is compared with a reference value (see Fig. 2.2). The difference is then amplified again to drive the z-piezo. The phase of the amplifiers is chosen to provide negative feedback: If the tunneling current exceeds the reference value, then the voltage applied to the z piezo tends to withdraw the tip from the sample surface, and vice versa. Therefore, an equilibrium z position is established through the feedback loop. As the tip scans over the xy plane, a two-dimensional array of equilibrium z positions, representing a contour plot of the equal tunneling-current surface, is obtained and stored.

The contour plot is displayed on a computer screen, either as a line-scan image or as a gray-scale image. The line-scan image is a sequence of curves, each of which represents a contour along the x direction with constant y. The curves with different heights are displaced vertically. The gray scale image is similar to a black and white television picture in the past,

but now it can be transformed to color scale like “red temperature”. The bright spots represent high z values, and the dark spots represent low z values.

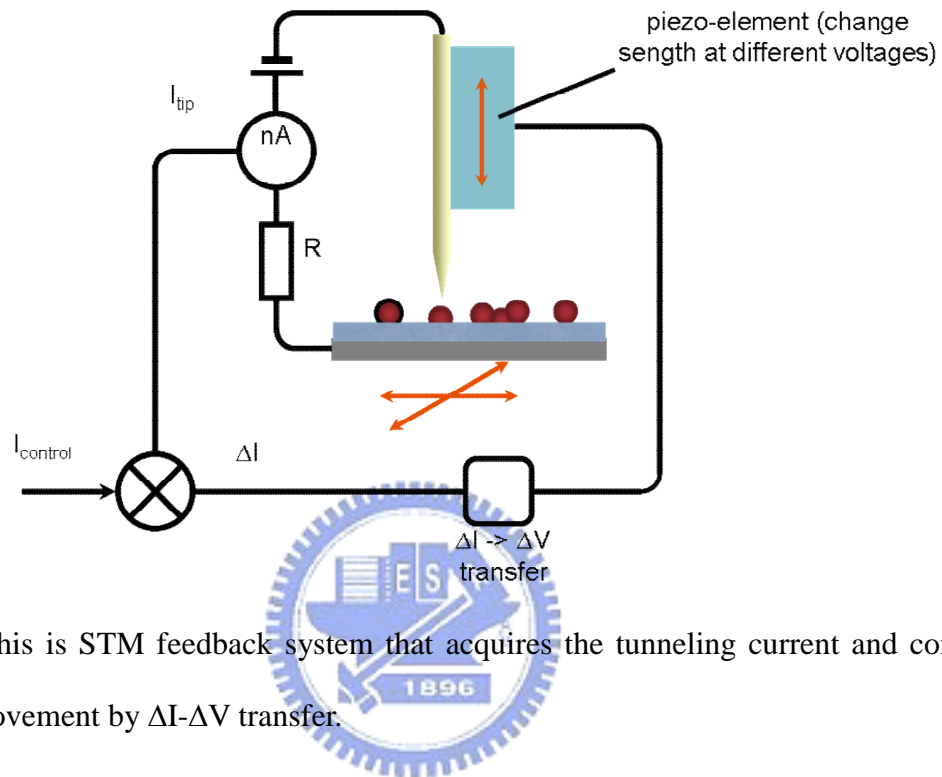


Fig. 2.2 This is STM feedback system that acquires the tunneling current and control the z-piezo movement by  $\Delta I$ - $\Delta V$  transfer.

### 2.2.3 Constant-current mode and constant-height mode

STM can image a sample surface in either constant-current mode or constant-height mode, as shown in the Fig. 2.3. In constant-current mode, in order to maintain the tunneling current constant, STM uses feedback to adjust the height of the scanner at each measurement point, for example, when the system senses a tunneling current increase, it adjusts the voltage applied to the piezoelectric scanner so that the scanner lifts the tip and increases the tip-sample distance. The scanner height measured at each location on the sample surface constitutes the topographical image. The constant-current mode is thus, generally used to acquire surface height data. The scanning is limited by the feedback response and thus, it slows down the process of imaging an irregular surface at a larger scan size. In constant-height mode, the tip scans at a constant height above the sample and the tunneling current changes due to the topography and the local surface electronic properties of the sample. The current image is a result of measured tunneling current at each location on the sample surface. The constant-height mode can acquire data faster because the system doesn't have to move the scanner in the vertical direction; therefore, it is most often used for imaging relatively smooth surfaces.

Technically, STM tunneling current is correlated to the surface electronic density of states, i.e., the number of filled or unfilled electron states near the Fermi level, within an energy range determined by the bias voltage. Therefore, STM measures constant tunneling probability instead of the physical topography of the surface. STM tunneling spectroscopy is a useful tool to study the electronic structure and property of a sample surface at the atomic level, the current-voltage relationship, a constant tip-sample distance or the current-distance relationship with a constant bias voltage.

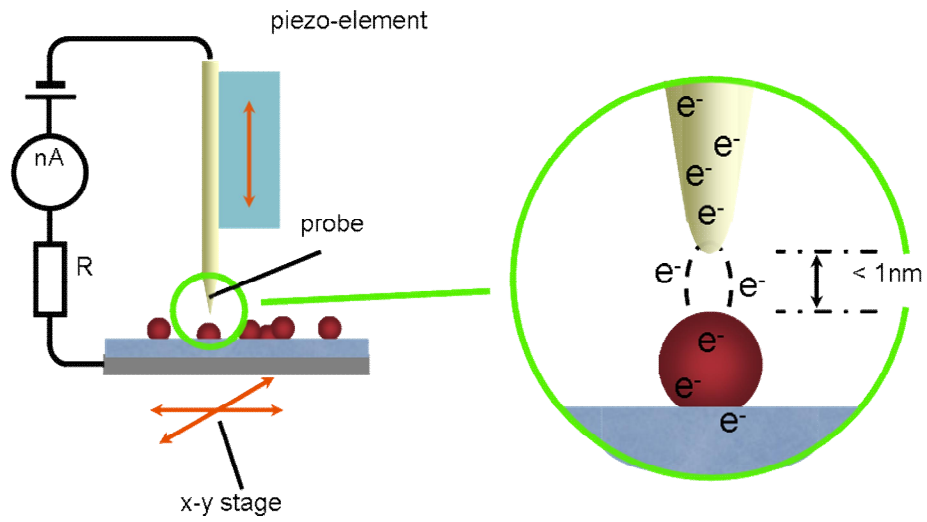
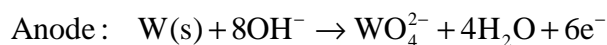
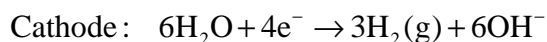


Fig. 2.3 STM operation and schematic diagram.



## 2.2.4 Preparing STM tips

STM tips are typically made from cut-to-size pieces of tungsten (W) wire. A standard method for STM tip fabrication is electro-chemical etching. This method has the advantage of being straight forward and easy to produce. A piece of W wire and a cylindrical stainless steel must reach the surface of the solution of 2M NaOH. The depth of W wire is 1.5~2 mm below the solution level. A positive voltage, 7 V, is applied to the W wire as the anode and the cylindrical stainless steel is as the cathode as shown in Fig. 2.4. Certain chemical reactions are expected:



At the interface of air and the solution, the chemical reactions occurred. A neck of the W wire forms at the surface and the immersed portion of the tip eventually fall off. Etching is usually stopped at this point by a feedback controller that senses the reduction in current. The tip is then washed with distilled water and can be used immediately or stored in an inert environment.

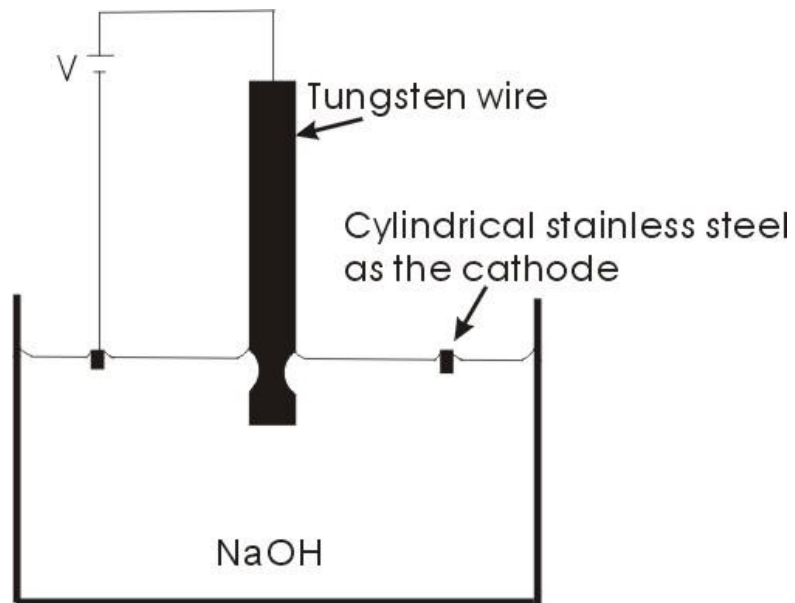
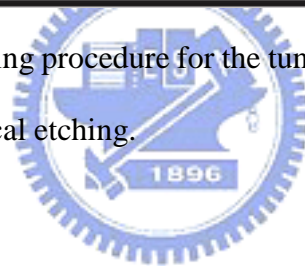


Fig. 2.4 The sketch of the etching procedure for the tungsten (W) tip. The atomic scale tip can be made by the electro-chemical etching.



## 2.3 Noncontact-Atomic Force Microscopy (NC-AFM)

### 2.3.1 Introduction

Short-Range atomic force is equally important in STM as the AFM. AFM was invented by Binnig *et al.*, utilizes these short-range forces to obtain surface topography of sample surfaces, down to atomic scale. Figure 2.5(a) demonstrates the force with distance dependency between tip and sample. The electrostatic force can be detected less than  $10^{-6}$  m, and vdW force less than  $10^{-9}$  m. They are the main parts for AFM work-interval. However, measurement of these tiny forces has been very different and was only possible in a very limited number of sample-tip configurations. Atomic resolution NC-AFM was finally achieved in 1995 using amplitude about 1-10nm for imaging and force spectroscopy.

Figure 2.5(b) illustrates the force as function of the tip-sample distance, and it shows two kinds of the active forces, repulsive and attractive. NC-AFM works with the attractive force between tip and sample, and it does not damage the surface. On the contact mode AFM is operated with repulsive force to detect Coulomb force between a tip and a sample, and it is destructive to the sample. Between contact and noncontact mode, the tapping mode AFM works between the repulsive and attractive forces. Comparison of these three modes, NC-AFM is becoming a popular tool as compared to others to obtain topography on these advantages.



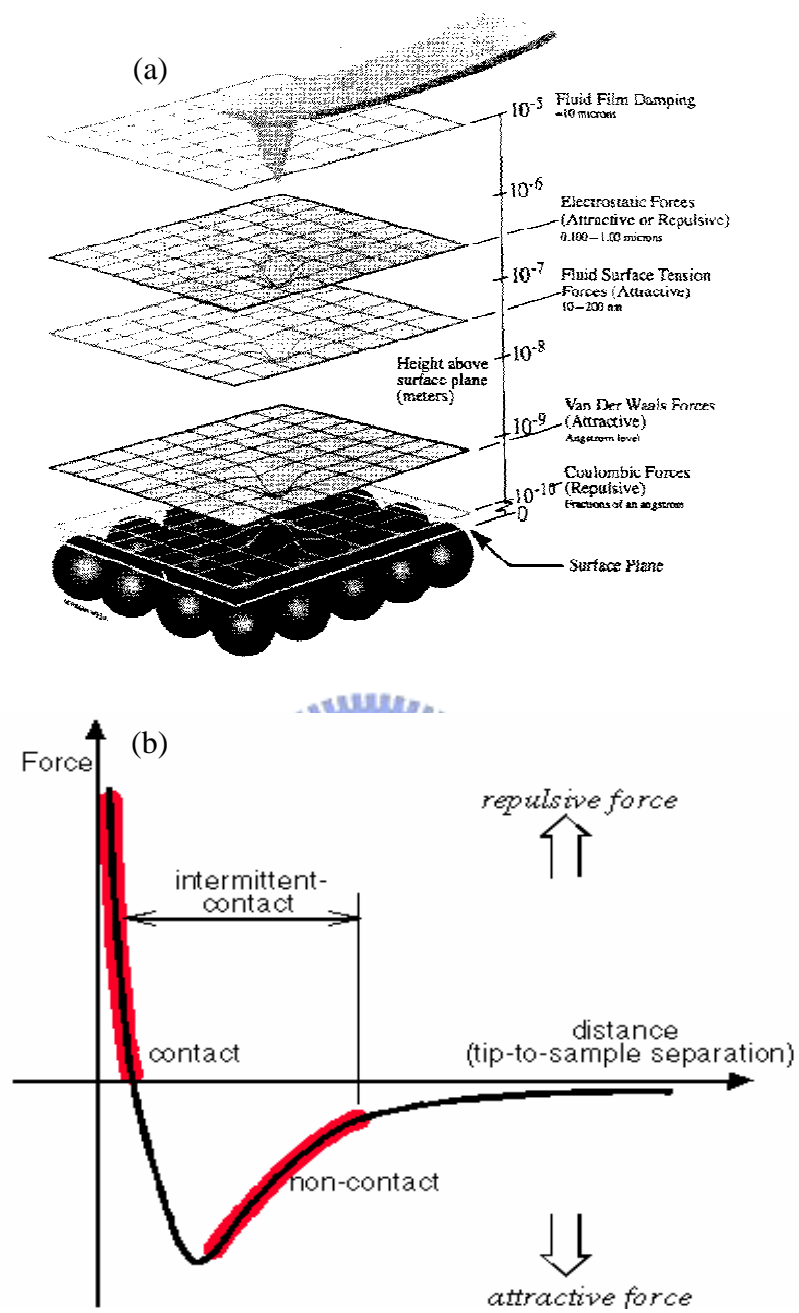


Fig. 2.5 (a) The effective distance for the different force. (b) Forces versus distance curve for different operation modes of AFM. Copied from internet.

## 2.3.2 Feedback system

In NC-AFM, the cantilever is driven by an ac bias ( $V_{ac}(f_0)$ ) to oscillate with a resonance frequency ( $f_0$ ). The AFM diagram is shown in Fig. 2.6. Adjust the laser point on the back of the cantilever and reflected to the Position Sensitive Detector (PSD). We can obtain the topography image by the feedback system to get a constant frequency shift between the tip and the sample.

Since the interaction force strongly depends on the tip-sample distance, this frequency shift can be used as feedback index for a distance regulation (z-loop) by lock-in amplifier as shown in Fig. 2.6. The interaction with the sample of the vibrating cantilever results in a shift of the cantilever resonance frequency ( $\Delta f$ ). In order to maintain the frequency shift ( $\Delta f$ ), the feedback control will approach or retract with the piezoelectric tube scanner. From the piezo movement of the z-axis, the topography can be acquired from the surface contour.

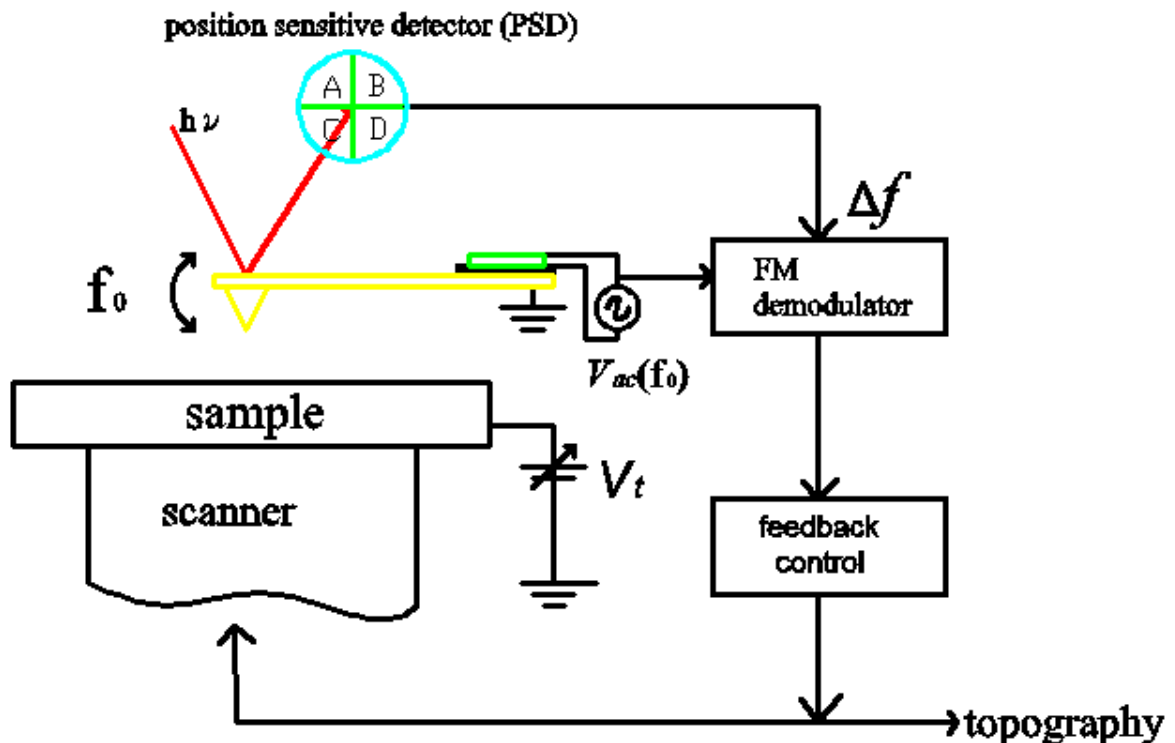


Fig. 2.6 AFM block diagram for getting the topography by the feedback system.

### 2.3.3 Light beam adjustment

The optical beam deflection technique used in the Omicron VT Beam Deflection AFM measures the deflection of the cantilever by detecting the deflection of a reflected light beam. A special infrared laser (wavelength: 850nm) is used as a light source. The light is not visible for the human eye. Thus, the supplied CCD camera is used for the alignment of the light beam.

The laser beam is generated in the Light Unit connected to the light Unit flange as illustrated in Fig. 2.7. In the figure, an optical fiber then passes the laser beam on through the base flange and up to the microscope stage. The beam positioning elements are mounted on and move with the coarse positioning drive.

The primary beam from the beam to the cantilever can be positioned in x-direction using a little micro slide and in y-direction using a rotatable mirror. We can tune the x and y direction of the laser point that was seen on the back of the cantilever in CCD camera. When the primary beam is correctly positioned, the mirror  $L_{\text{PSD}}$  may be used for optimizing the position of the secondary beam on the position sensitive detector (PSD). The PSD yields variety of signals. Initially, i.e., without any forces applied, the secondary beam should be positioned in the centre of the detector. A normal force signal moves the reflected beam vertically, and a lateral force signal horizontally across the PSD.

Note that the vertical difference is independent of the horizontal position of the beam and vice versa. In addition, the initial positioning of the beam is not binding; however, if the offset exceeds, it may reduce the detection range and linearity. For convenience, the horizontal position of the beam has been pre-adjusted in the factory to a close-to-zero position. Thus, in order to compensate for manufacturing tolerances, the secondary beam can be adjusted vertically via mirror  $L_{\text{PSD}}$ .

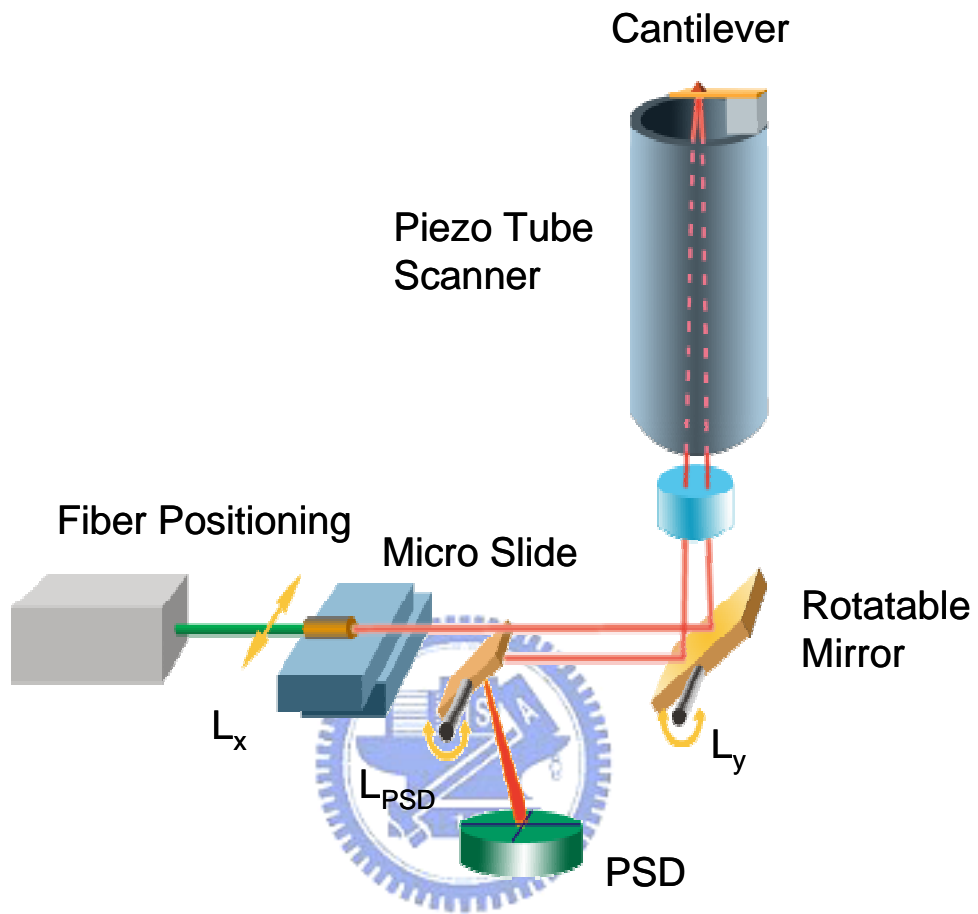


Fig. 2.7 Schematic diagram of the optical beam deflection. AFM deflection beam is adjusted on the position sensitive detector (PSD).

## 2.3.4 The measurement of the spectroscopy

### (a) Measurement of $Z(V_t)$

The height displacement as functional as tip applied bias  $Z(V_t)$  in specific frequency shift measured on the surface as demonstrated in Fig. 3.8. For getting the  $Z(V_t)$ , we set the variation range of the applied bias on the tip, and then selected the specific area on the sample. The cantilever moved to the specific area, and obtained the height variation with the change of the applied bias.

The minimum of the curve for  $Z(V_t)$  illustrates the compensated position for the material, and different materials have individual minimum position. If the contact potential needs to be compensated, the minimum value of the tip bias should be applied, and the electrostatic force can be canceled between tip and sample. Furthermore, in order to get correct height for these two materials, the applied bias on tip will be changed to the middle of the sum of these minimum values.

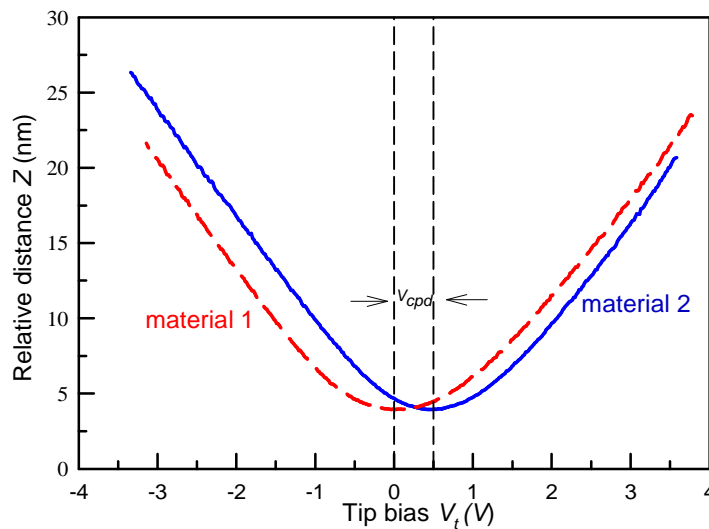


Fig. 2.8 Demonstration of the voltage dependence of the height displacement  $Z(V_t)$  for two different materials on the surface. The contact potential difference ( $V_{cpd}$ ) can be acquired from the maximum point of the material 1 (red-dash line) and the material 2 (blue-solid line).

## (b) Measurement of $\Delta f(V_t)$

To monitor the electrostatic interaction, frequency versus bias-voltage curves were recorded at the constant tip-sample distances: First, a few images in constant frequency shift were observed on the different material surface to reveal whether the tip is stable. Then the scanning process and the distance controller were interrupted and a frequency shift versus the applied tip bias curve ( $\Delta f(V_t)$ ) [21] were measured by the setpoint frequency shift ( $\Delta f$ ) with the feedback off as shown in Fig. 2.9. From the maxima of these curves, the contact potential difference between the material1 and the material2 could be defined as  $V_{cpd} = 0.5$  V. It was determined to be constant and consistency between these two materials.  $\Delta f(V_t)$  and  $Z(V_t)$  can get the contact potential difference, but  $\Delta f(V_t)$  is easy to crash tip than  $Z(V_t)$ . In this research, we prefer use  $Z(V_t)$  instead of  $\Delta f(V_t)$ .

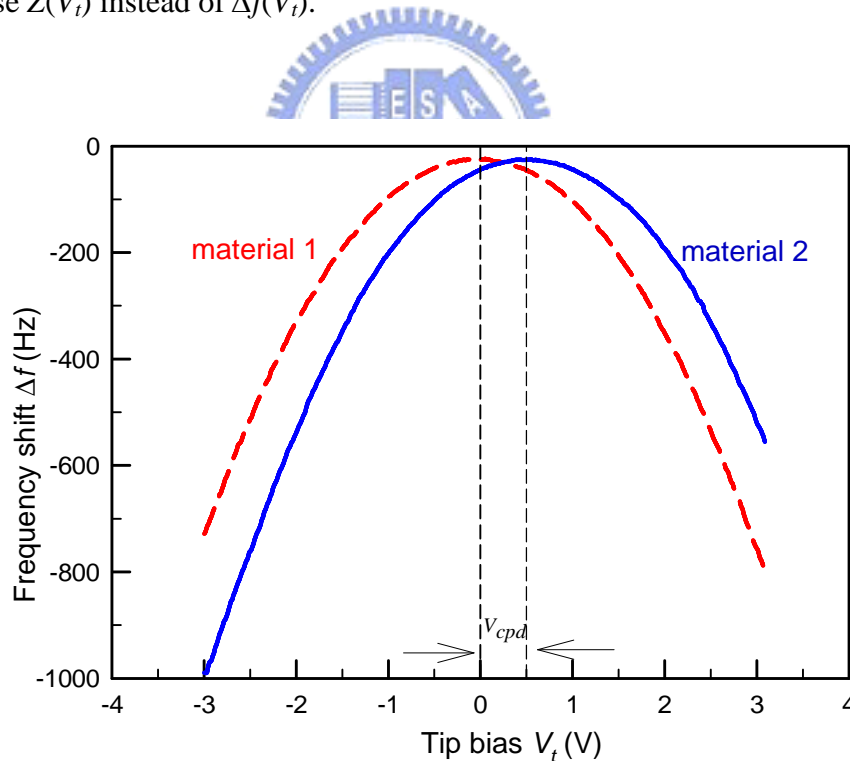


Fig. 2.9 Illustration of the voltage dependence of the frequency shift for two different materials on the surface. The contact potential difference ( $V_{cpd}$ ) can be acquired from the maximum point of the material 1 (red-dash line) and the material 2 (blue-solid line).

### (c) Measurement of $Q(z)$ and $\Delta f(z)$

True tip-sample distance can be determined by using a compensated bias to sample when cantilever was scanning over the surface from the measurement of the damping variation and frequency shift as function as tip-sample distance ( $Q(z)$  and  $\Delta f(z)$ ) [22,23,24]. The  $Q(z)$  and  $\Delta f(z)$  were measured simultaneously by controlling the piezoelectric tube scanner of cantilever to forward the sample in feedback off. Figure 2.10 shows the damping variation was almost constant up (red square) to contact point (zero point) and then quickly increased with decreasing tip-sample distance. An increase in the damping variation means an increase in the energy loss of the oscillating cantilever as a result of the cyclic repulsive contact between the tip and the sample surface. Therefore, the increasing point is defined as contact point (zero point) between the tip and the surface. Hence, regions I and II are the noncontact- and the cyclic-contact regions, respectively. On the contrary, the  $\Delta f(z)$ , first gradually and then quickly, decreased (region I) and became a minimum at point A.

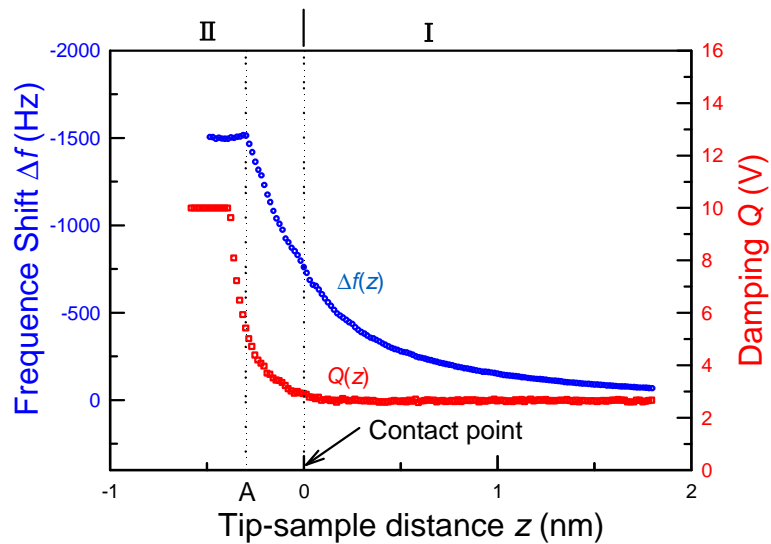


Fig. 2.10  $\Delta f(z)$  shows approaching trace of the frequency shift of the cantilever and  $Q(z)$  shows the simultaneously measured by the piezoelectric tube scanner as a function of tip-sample distance  $z$ . The distance dependence of the frequency shift reverses at point A. Contact occurs at  $z = 0$  nm where the damping starts to increase.

### 2.3.5 Preparing AFM cantilevers

The AFM tip-cantilever assembly is normally manufactured as unit micro mechanically to past the cantilever on the cantilever holder. For this experiment, purchase of Si-cantilever and PtIr5-cantilever was produced from a vendor and utilized. For Si-cantilever, it is a heavily n-dopant, thus the Si-cantilever is conductive but normally a native silicon oxide that forms on the cantilever. For PtIr5-cantilever, it is evaporation with a thin PtIr layer (~30nm) on the cantilever. However, this process deteriorates the tip geometry and such cantilever can only kept in air for a few days before the metal surface becomes too contaminated before the experiments.

Cantilevers must be mounted to the cantilever holder using vacuum compatible epoxy cement. Fix the cantilever holder to the attaching device as shown in Fig. 2.11. Place the cantilever chip onto the cantilever holder. Position the cantilever using a magnifying glass or microscope and clamp it provisionally. Finely adjust the cantilever while checking with the microscope on the right position. Then, attach the cantilever chip onto the tip holder, and wait until the cantilever chip is firm onto the tip holder. The cantilever must be carefully taken out from the attached device, and loads onto the UHV system.

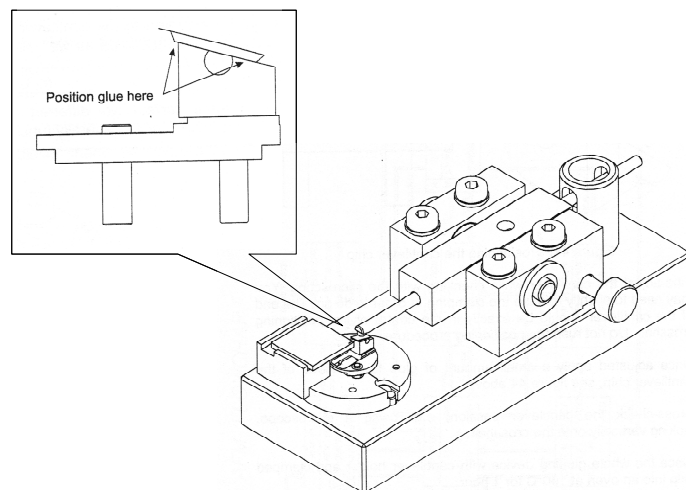


Fig. 2.11 OMICRON attaching device and positioning the cantilever chip.